Calculated equilibrium properties, electronic structures and structural stabilities of Th, Pa, U, Np and Pu

Calculated equilibrium properties, electronic structures and structural stabilities of Th, Pa, U, Np and Pu

M Pénicaud

Commissariat à l'Energie Atomique, DAM–Île de France, BP 12, 91680 Bruyères-le-Chatel, France

Abstract. With the FPLAPW (full potential linearized augmented plane wave) method we calculate the equilibrium volumes, the bulk moduli and the electronic structures of the light actinide metals in their crystal structure of ambient conditions. We examine also their structural stability under pressure and we show several phase transitions for Np and Pu. The results are significantly different from the previous calculations. With our fully relativistic MTO (muffin tin orbital) method we find for the stabilized δ-phase (face centred cubic) of Pu an electronic structure which presents a 5f peak pinned at the Fermi level, in agreement with photoelectron spectroscopy and the high value of the electronic specific heat coefficient.

1. Introduction

In a previous study [1] ground-state properties of the whole series of actinide metals are investigated by means of total-energy calculations in the local density approximation (LDA) using a fully relativistic muffin-tin orbital band structure method (MTO). With the experimental equilibrium volumes, quite a good agreement is obtained from Ra to Pu with the usual LDA scheme. A face centred cubic (fcc) crystal structure is used for all the calculations instead of the, in some cases, much more complex crystal structure: Ra is body centred cubic (bcc), Ac and Th are fcc but Pa is body centred tetragonal (bct), U is orthorhombic with two atoms in the unit cell (ort2), Np is orthorhombic with eight atoms in the unit cell (ort8) and Pu is monoclinic with 16 atoms in the unit cell (mono16).

To obtain reliable theoretical equilibrium volumes in open structures such as orthorhombic or monoclinic it is necessary to perform full-potential calculations; this has been done previously with a full-potential linear muffin-tin orbital (FPLMTO) code for Pa, U, Np and Pu [2]. Here we present the results obtained with a full-potential linear augmented plane wave (FPLAPW) code [3]. These two full-potential codes are fully relativistic for the core states and semi-relativistic with variational treatment of spin–orbit coupling for the valence band; they also use the generalized gradient approximation (GGA) for the exchange–correlation energy functional but we take a more recent formulation [4] than the one [5] used with FPLMTO. In all calculations the semi-core states 6s and 6p in the valence band have been taken account of.

Very recently the equilibrium volumes of light actinide metals have been calculated with the FPLAPW code of Singh [6]. The formulation [5] of the GGA as in FPLMTO is used. We also compare these results with ours.

The δ phase of Pu (fcc) is not stable at ambient condition. Its stability is obtained by a special electronic structure with semi-localized 5f electrons which occurs at temperature

between 583 K and 725 K or at ambient conditions by the addition of a small amount of Ga (or Am, Al, Ce,...). Here we present an electronic structure slightly different from the one suggested in [1]; it gives the correct equilibrium volume in the δ phase and a better agreement with experiments.

2. Methods of calculation

With our MTO method [1] the solid is modelled by spheres of volume equal to the crystal cells; inside each sphere the potential has spherical symmetry. This atomic sphere approximation (ASA) is well suited for the compact, cubic and hexagonal, crystalline structures. The one-electron MTO wave functions on the crystal lattice are linear combinations of the exact solutions ϕ of the Dirac equation in the spherical potential. The coefficients are solutions of a linear homogeneous system involving logarithmic derivatives of the wave functions ϕ on the atomic sphere and 'structure constants' that only depend on the type of crystal lattice considered.

In the FPLAPW method [3, 7] there is no approximation on the crystal geometry but the wave functions are only variational approximations of the true wave functions obtained in the region of fixed energies E_ν. Also the relativistic effect of spin–orbit coupling is not solved by the Dirac equation but is incorporated for the valence electrons at the second-variational level [7], in which the effects of spin–orbit coupling are treated perturbatively in a set of scalar-relativistic orbitals found within an energy window of specified width. This procedure is rigorously adapted only for a small spin–orbit coupling.

In the LAPW method the crystal is divided into two regions: (I) 'muffin-tin' spheres centred on the ions where the potential has very strong variations and (II) an interstitial zone where the potential is almost constant. The spin–orbit coupling is considered only inside the atomic spheres; consequently the results may depend on these sphere radii.

In the 'full-potential' method the potential $V(\vec{r})$ and the electronic density $\rho(\vec{r})$ are not limited to their spherical component but are taken in the following form:

$$V(\vec{r}) = \begin{cases} \displaystyle\sum_{lm} V_{lm}(r) Y_{lm}(\hat{r}) & \text{inside (I)} \\ \displaystyle\sum_{\vec{K}} V_K \, \mathrm{e}^{\mathrm{i}\vec{K}\vec{r}} & \text{inside (II)} \end{cases}$$

where the $Y_{lm}(\hat{r})$ are spherical harmonics.

During the self-consistent cycle, the integration over the Brillouin zone is performed using 'special-point' sampling [8]. To obtain a good convergence on the total energy we take in the irreducible part of the Brillouin zone (iBZ) 44 points in the bcc structure, 47 points in fcc and 99 points in bct, which yield each time 1000 points in the whole Brillouin zone (wBZ). In hcp (hexagonal close packed, ideal c/a ratio, two atoms in the unit cell) we take 42 points in the iBZ yielding 500 points in the wBZ, in ort2 (α-U) 75 points in the iBZ yielding 405 points in the wBZ, in ort8 (α-Np) 18 points in the iBZ yielding 144 points in the wBZ and in mono16 (α-Pu) 15 points in the iBZ yielding 60 points in the wBZ. However the more atoms a crystal cell contains, the fewer points are necessary for the integration over the wBZ which is smaller. We verify that the number of points in the wBZ multiplied by the number of atoms in the crystal cell gives about 1000 points. We have also studied the β high temperature phase of Np which is tetragonal with four atoms in the unit cell; we take 24 points in the iBZ yielding 175 points in the wBZ. Finally, a special hexagonal structure has been observed at high pressure in Pu [9] which contains eight atoms in the unit cell (hex8): we take for it 15 points in the iBZ corresponding to 125 points in the wBZ.
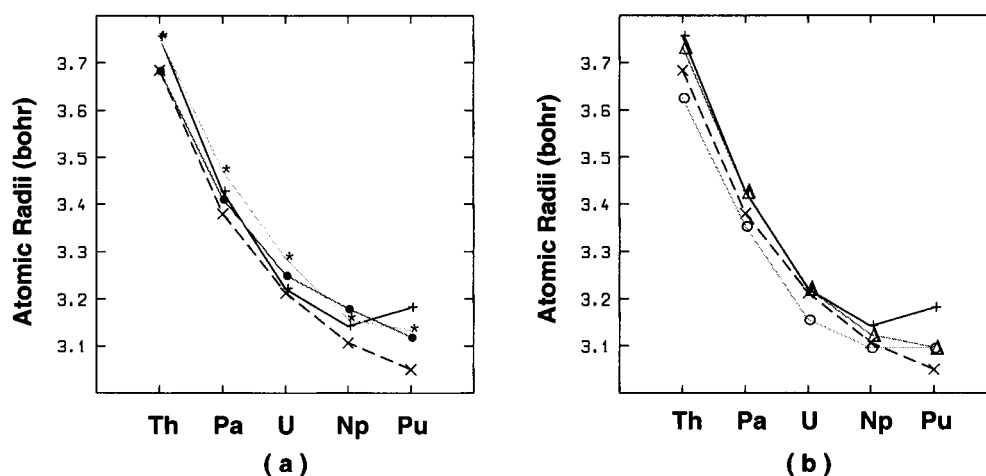
Figure 1. A comparison of experimental (+) and theoretical equilibrium atomic radii. (a) Calculations by MTO (∗) and FPLAPW (●) in the fcc structure and by FPLAPW (×) in the real crystal structures (Th fcc, Pa bct, U ort2, Np ort8, Pu mono16) (b) Calculations in the real crystal structures by FPLMTO (○), our FPLAPW (×) and Singh's (△).

3. Equilibrium properties

In figure 1(a) we compare the experimental [10] Wigner–Seitz atomic radii with the ones calculated by MTO [1], with the Kohn–Sham (KS) exchange–correlation [11] in the fcc structure, and by FPLAPW [3] with the GGA exchange–correlation in the fcc and the real crystal structures. We also compare, in figure 1(b), the experimental data with the values calculated in the real crystal structures by FPLMTO [2], our FPLAPW [3] and Singh's [6]. During our search for the equilibrium volumes, the internal crystallographic parameters and the axial ratios c/a, b/a for the α-Pu, α-Np, α-U and α-Pa structures are kept constant at the experimentally determined values at ambient temperature and pressure [10].

In figure 1(a) we notice for Th, which is fcc, that the agreement with the experimental equilibrium radius is better with MTO than with FPLAPW, but for α-U we obtain exactly the experimental value with FPLAPW.

In figure 1(b) we see that the results obtained with Singh's FPLAPW for Th, Pa and U are the closest to the experimental data. This has been argued to be due to a better choice of the muffin-radii [12].

The calculated values with FPLMTO [2] are similar to ours, but the agreement between theory and experiment for α-U is better in our case. On the other hand, for α-Pu FPLMTO gives an equilibrium volume which is not less than the one calculated for α-Np in agreement with experiment. Neither our FPLAPW code nor Singh's reproduces this effect.

In figure 2 we compare the experimental bulk moduli [9, 13] to the ones calculated by MTO [1] and FPLAPW in the fcc structure and by FPLMTO [2] and FPLAPW in the real crystal structures. If the bulk moduli are calculated at the theoretical equilibrium volumes we see for Th, which is fcc, an excellent agreement between theory and experiment whatever method is used; in contrast for Pa, U, Np and Pu the agreement is poor except for α-U where our FPLAPW gives the experimental value. These differences can be explained because generally theoretical and experimental volumes are different; this is why we have also calculated the bulk moduli at the experimental equilibrium volumes: the results are specially better for Pu.
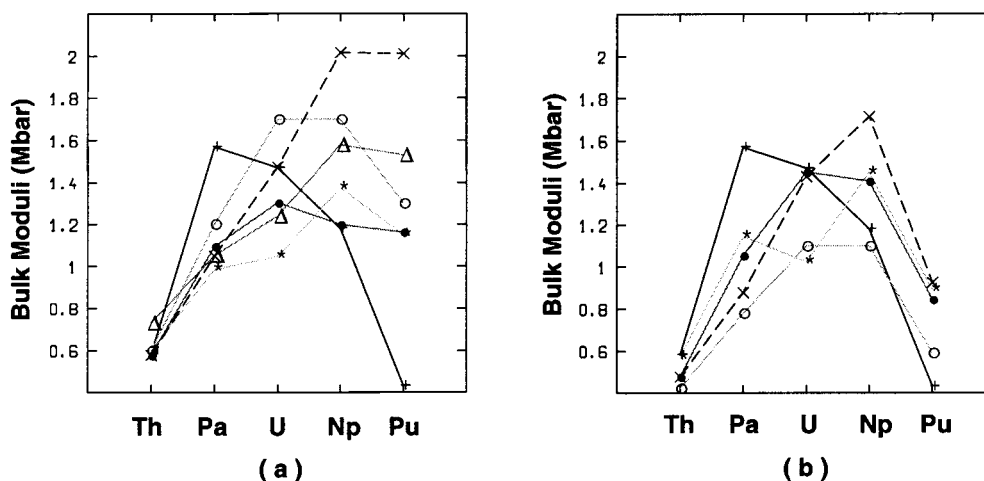
Figure 2. Experimental (+) and theoretical bulk moduli. The theoretical bulk moduli are calculated at the values of the theoretical (a) or experimental (b) volumes. Calculations by MTO (∗) and FPLAPW (●) in the fcc structure and by FPLMTO (○), our FPLAPW (×) and Singh's (△) in the real crystal structures (Th fcc, Pa bct, U ort2, Np ort8, Pu mono16).

Another important reason for the discrepancies is that we have not optimized theoretically the various crystallographic parameters of the complex structures.

4. Electronic structures

In figures 3–5 we show the calculated densities of states (DOSs) by FPLAPW, at the values of the experimental equilibrium volumes for fcc Th, bct Pa, α-U, α-Np and α-Pu. For Th we obtain them also by MTO and they look similar. With MTO we can differentiate the $5f_{5/2}$ and $5f_{7/2}$ partial DOS; this is not possible with FPLAPW which does not use the Dirac equation. By FPLAPW the DOSs are calculated by means of the modified tetrahedron method [14] and then convoluted with a Gaussian function of width 0.05 eV. By MTO the energy of each state calculated is broadened by a Gaussian of width 0.05 eV to obtain the DOS [15]. Our DOSs are similar to those previously computed by FPLMTO for the α-phases of Th, Pa, U [16], Np [17] and Pu [2, 32].

With the value of the density of states $D(E)$ at the Fermi energy E_F it is possible to calculate [18] the electronic specific heat coefficient γ:

$$\gamma = \frac{\pi^2}{3} k_B^2 D(E_F)$$

where k_B is the Boltzmann constant. The results are compared with experiments [19] in figure 6, where we can see that the agreement is not very good.

5. Equilibrium properties and electronic structure of δ-Pu

Here we present an electronic structure obtained with our MTO method for δ-Pu, slightly different from the one suggested in [1] but based on the same principle. Since LDA is known to overestimate the extent of the localized orbitals and hence the effects of interatomic hybridization and overlap, we neglect these terms in the matrix elements. We reproduce the
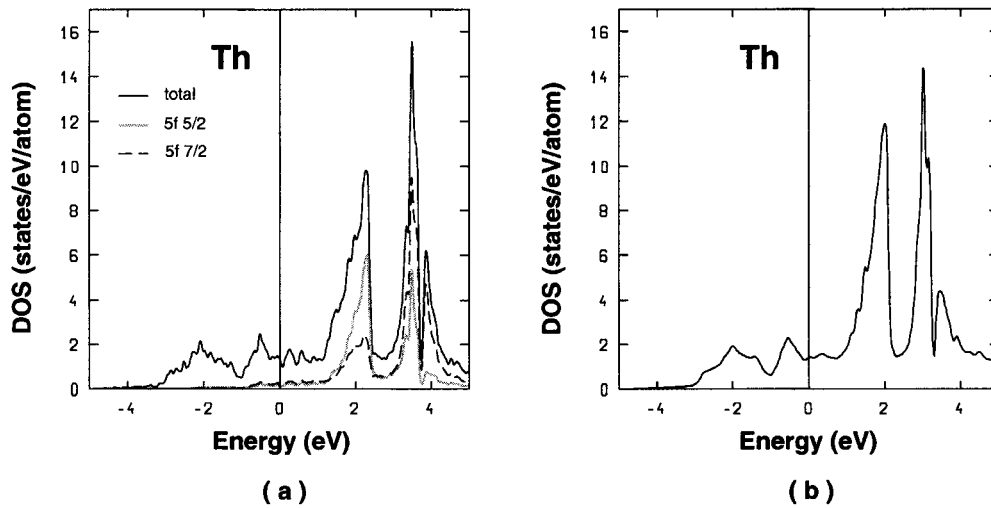
Figure 3. Densities of states for fcc Th calculated by MTO (a) and by FPLAPW (b) at the value of the experimental equilibrium volume. They are smoothed by a Gaussian function of width 0.05 eV. Energies are relative to the Fermi energy.
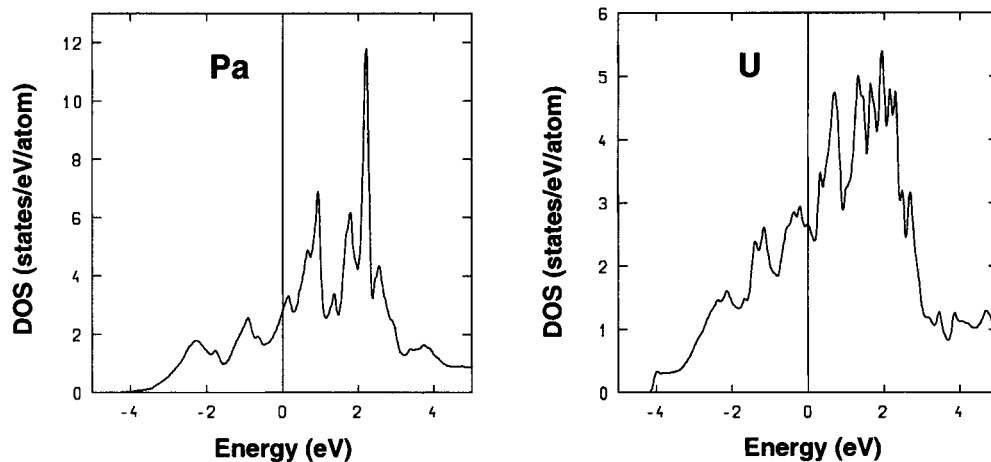

Figure 4. Densities of states for bct Pa and ort2 U calculated by FPLAPW at the values of the experimental equilibrium volumes. They have been convoluted with a Gaussian function of width 0.05 eV. Energies and relative to the Fermi energy.

localized character of electrons by removing the coupling between their states and other angular momenta. To do this using the MTO method, we only have to cancel the corresponding matrix elements in our 'structure constants'.

For Am, Cm, Bk and Cf good agreements with the experimental equilibrium volumes and the bulk moduli were obtained by removing the coupling between the 5f and the s, p, d electrons. For Es removing in addition the coupling of the 6d with the s, p electrons produces also an excellent agreement with the experimental equilibrium volume.

For δ-Pu we have now improved out initial choices. As proposed in [1] only the $5f_{5/2}$ electrons are uncoupled from the s, p, d electrons and we use the KS exchange–correlation. In addition we reduce also, by a small fraction, the coupling of the $5f_{5/2}$ with the $5f_{7/2}$ electrons
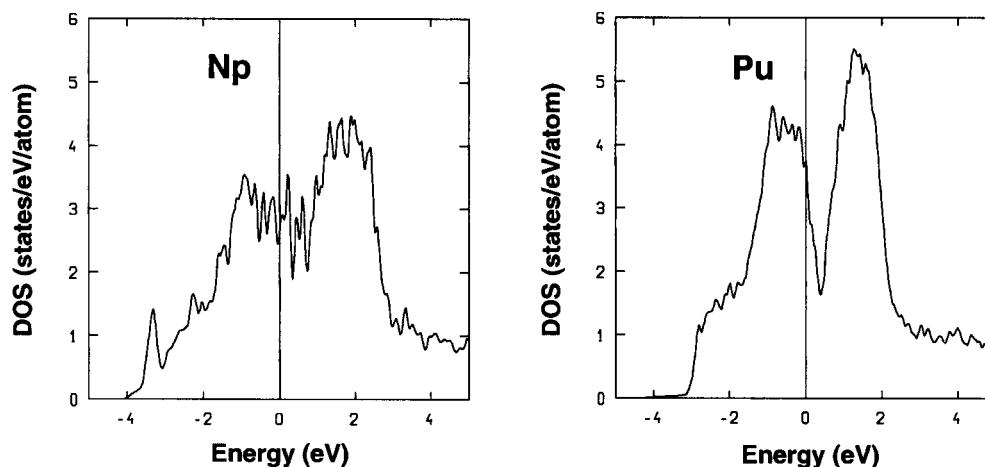
Figure 5. Densities of states for ort8 Np and mono16 Pu calculated by FPLAPW at the values of the experimental equilibrium volumes. They have been convoluted with a Gaussian function of width 0.05 eV. Energies are relative to the Fermi energy.
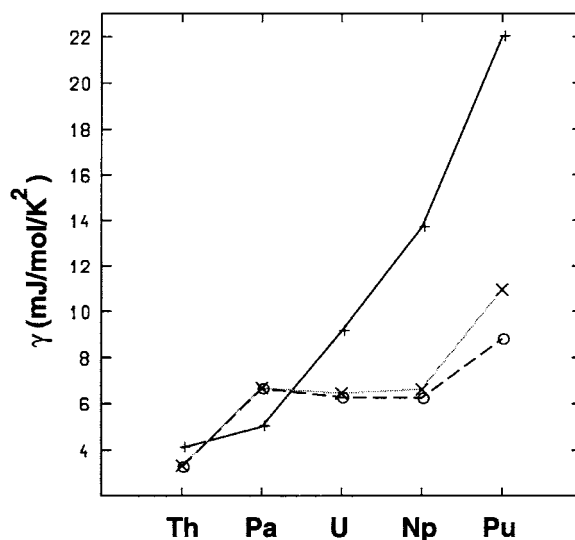

Figure 6. A comparison of the electronic specific heat coefficient (γ) experimental (+) values to those calculated with the DOS at E_F obtained at the experimental equilibrium volumes with FPLAPW. (O), DOS smoothed by a Gaussian function of width 0.05 eV; ($\times$), DOS without smoothing.

by multiplying the corresponding MTO 'structure constants' by 0.954. This way we obtain the correct δ-phase equilibrium volume (24.93 Å^3, 168.24 bohr^3) and for the bulk modulus 557 kbar instead of the experimental 299 kbar [20].

Our calculated DOSs show (figure 7) a 5f$_{5/2}$ peak pinned at the Fermi level in agreement with photoelectron spectroscopy experiments performed at ITU Karlsruhe (Germany) [21] and more recently at Los Alamos (USA) [22].

Our calculated coefficient of electronic specific heat $\gamma = 45$ mJ mol^{-1} K^{-2} is also in good agreement with the very high experimental value, 53 mJ mol^{-1} K^{-2} [19]. γ is proportional to
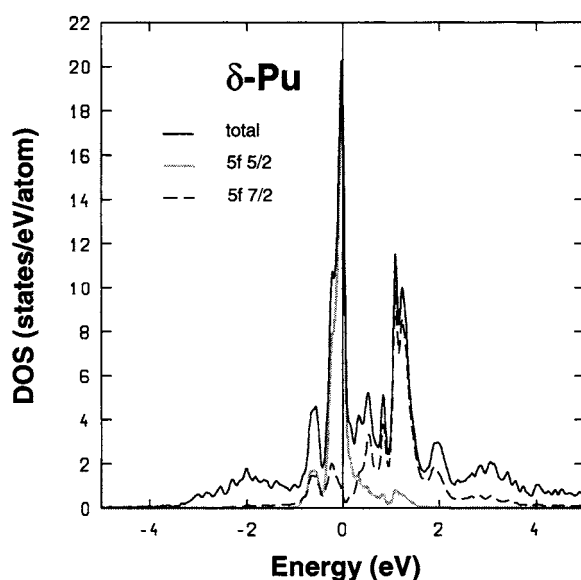
Figure 7. Densities of states for δ-Pu. Energies are relative to the Fermi energy.

the density of states $D(E)$ at the Fermi energy E_F and its high experimental value is due to the $D(E)$ peak at E_F.

Recently other attempts have been made to model the δ-phase of Pu. The SIC–LSD method [23] succeeded in reproducing the localization effects in the lanthanides [24] and the last actinides (Am to Es) [25] but failed in the case of δ-Pu [25]. With the LDA+U method [26], treating U as an adjustable parameter, it has been possible to obtain the correct equilibrium density [27–29], but the bulk modulus of 610 kbar found in [28] is worse than ours and principally the calculated DOSs [28] show no 5f peak at E_F, inconsistent with the photoelectron spectroscopy experiments; consequently the γ of 8.7 mJ mol^{-1} K^{-2} which can be deduced from [28] is far too low. This would be the same for the calculations performed in [29] where the 5f electrons are also swept out of the valence band. Eriksson *et al* [30] constrained four 5f electrons to be in the core, letting only one remain in the conduction band, and they obtained, with the FPLMTO method, the experimental equilibrium density of δ-Pu, but again the calculated DOSs [30] show no 5f peak at E_F and the deduced γ of 5.2 mJ mol^{-1} K^{-2} is ten times too low.

6. Structural stability of Np

The comparison of total energies calculated in different crystal structures tell us the most stable and possible phase transitions.

For Np we compare in a wide volume range (figure 8) the energies, calculated with FPLAPW, in the following structures: α-Np (ort8), β-Np (high temperature structure of Np which is tetragonal with four atoms in the unit cell, t4), bcc and fcc. The internal crystallographic parameters and the axial ratios c/a, b/a are kept constant at the experimental determined values for the α-Np structure at ambient temperature (aT) and pressure (aP) [10] and for the β-Np structure at 313 °C, aP [10].

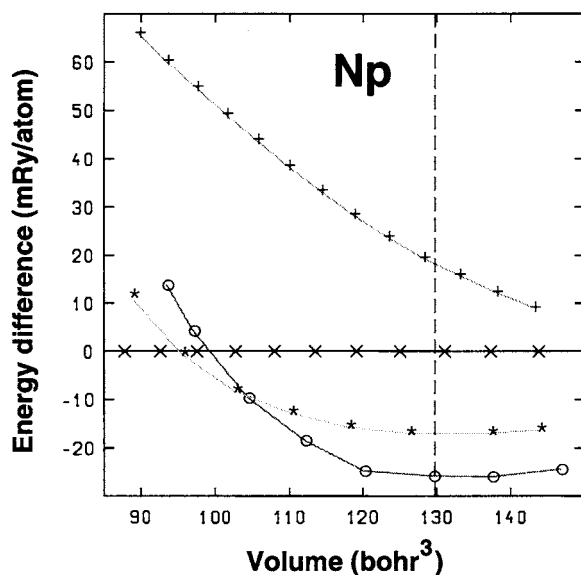At ambient pressure the α-Np phase is correctly found to be the most stable; two phase transitions follow:

$$\alpha\text{-Np} \rightarrow \beta\text{-Np} \rightarrow \text{bcc}.$$
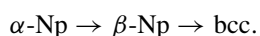
Figure 8. Total energy differences for Np, calculated by FPLAPW in the α-Np ($\bigcirc$), β-Np (*) and fcc (+) crystal structures, relative to the bcc ($\times$) structure, as functions of volume. The room-temperature equilibrium volume for Np is denoted by a vertical broken line.
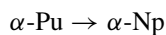
By FPLMTO [2, 31] the same sequence was obtained but the calculated transition pressures ($P_{\alpha \to \beta} = 140$ kbar, $P_{\beta \to bcc} = 570$ kbar) are clearly lower than ours. FPLMTO gives the α-Np $\to$ β-Np transition for a 10% compression (($V_0 - V$)/V_0, where V_0 is the experimental equilibrium volume) of Np; we find this later for a 19% compression of this metal.

Experimentally no phase transition was observed in Np below 520 kbar at ITU Karlsruhe [13].

7. Structural stability of Pu

We compare in a wide volume range (figure 9) the total energies, calculated with FPLAPW for Pu, successively in the α-Pu, α-Np, β-Np, bcc, hex8-Pu, fcc and hcp crystal structures. hex8-Pu is a hexagonal structure with eight atoms in the unit cell which was found under pressure at ITU Karlsruhe [9]. The internal crystallographic parameters and the axial ratios c/a, b/a are kept constant at the experimentally determined values for the α-Pu, α-Np structures at aT, aP [10], for the β-Np structure at 313 °C, aP [10], and for the hex8-Pu structure at aT, 550 kbar [9].

At ambient pressure the α-Pu phase (mono16) is correctly obtained to be the most stable but the energy different from the α-Np (ort8) phase is very small; consequently we have very soon, under pressure, the phase transition

$$\alpha\text{-Pu} \to \alpha\text{-Np}$$

which is followed later by two others:

$$\alpha\text{-Np} \to \beta\text{-Np} \to \text{bcc}.$$
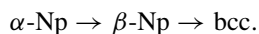
By FPLMTO [2, 32] the same sequence was obtained with lower transition pressures; FPLMTO gives the β-Np $\to$ bcc transition for a 20% compression (($V_0 - V$)/V_0) of Pu; we find it later for a 34% compression of this metal.
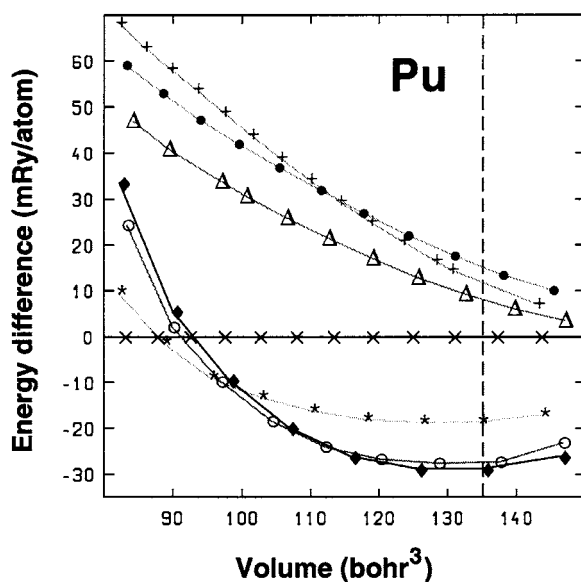
Figure 9. Total energy differences for Pu, calculated by FPLAPW in the α-Pu ($\blacklozenge$), α-Np ($\bigcirc$), β-Np (*), hex8 ($\triangle$), fcc (+) and hcp ($\bullet$) crystal structures, relative to the bcc ($\times$) structure, as functions of volume. The room-temperature equilibrium volume for Pu is denoted by a vertical broken line.
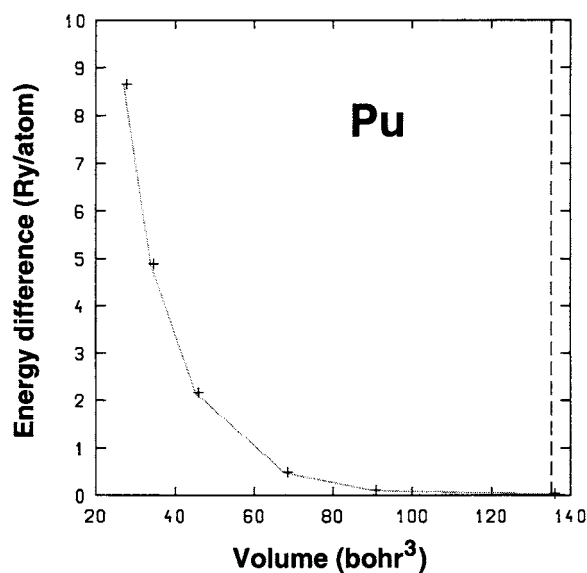

Figure 10. Total energy differences for Pu, calculated by MTO, in the fcc (+) crystal structure relative to the bcc structure, as functions of volume. The room-temperature equilibrium volume for Pu is denoted by a vertical broken line.

Experimentally at ITU Karlsruhe Pu was compressed in a diamond anvil cell up to 620 kbar [9], only one phase transition was observed at about 400 kbar, α-Pu $\rightarrow$ hex8-Pu. Theoretically the energy of the hex8-Pu phase stays always greater than the energies of α-Pu,

α-Np, β-Np and bcc phases and no transition to the hex8-Pu phase occurs in our domain of study, i.e. until a 40% compression of Pu. Therefore theory and experiment disagree for Pu.

Many approximations have been made in the FPLMTO calculations and ours. The FPLMTO and FPLAPW are variational methods, energy bands are obtained by linearization around fixed energies and there is a dependence in their choice. In the same way, there is a dependence in the choice of the muffin-tin radii [12]. Another approximation concerns the treatment, also variational, of the spin–orbit coupling, which is certainly insufficient in the Pu case.

Our MTO method is not variational and the relativistic effects are correctly treated by the Dirac equation; however it uses the ASA approximation, which is fair for the compact structures fcc and bcc. In figure 10 we can see on a very wide volume range that the bcc total energy is always lower than the fcc energy.

Therefore there is an agreement, at least theoretically, between FPLMTO, FPLAPW and MTO, to find the high pressure phase of Pu as bcc.

8. Conclusions

The results obtained with FPLAPW (Wein97 code) [3] for the equilibrium volumes, the bulk moduli and the structural stability of the light actinide metals are significantly different from the previous calculations with FPLMTO [2] and Singh's FPLAPW [6]. This shows some dependences in the various parameters of these methods, such as the choices of the exchange–correlation functional, of linearization energies, of muffin-tin radii and the truncations of basis and other expansions, which oblige us to be cautious about the results calculated. This is emphasized by some discrepancies with the experimental data. Nevertheless these methods are successful on many points such as obtaining theoretically the stability of the α crystal phases at ambient conditions.

We have calculated with our MTO method [1] an electronic structure of the stabilized δ-Pu in agreement with photoelectron spectroscopy and the high value of the electronic specific heat coefficient. However the understanding of the stability of the δ-phase at ambient temperature requires the direct determination of the effect on the electronic structure of the δ-phase stabilizers (Ga, Al, Am, Ce,...).

References

[1] Pénicaud M 1997 *J. Phys.: Condens. Matter* **9** 6341
[2] Söderlind P 1998 *Adv. Phys.* **47** 959
[3] Blaha P, Schwarz K and Luitz J 1999 *Wien97* Vienna University of Technology (an improved and updated version of the original Wien code Blaha P, Schwarz K, Sozantin P and Trickey S B 1990 *Comput. Phys. Commun.* **59** 399)
[4] Perdew J P, Burke S and Ernzerhof M 1996 *Phys. Rev. Lett.* **77** 3865
[5] Perdew J P, Chevary J A, Vosko S H, Jackson K A, Pederson M R and Singh D J 1992 *Phys. Rev.* B **46** 6671
[6] Jones M D, Boettger J C, Albers R C and Singh D J 2000 *Phys. Rev.* B **61** 4644
[7] Singh D J 1994 *Planewaves, Pseudopotentials and the LAPW Method* (Boston: Kluwer)
[8] Chadi D J and Cohen M L 1973 *Phys. Rev.* B **8** 5747
[9] Dabos-Seignon S, Dancausse J P, Gering E, Heathman S and Benedict U 1993 *J. Alloys Compounds* **190** 237
[10] Wyckoff R W G 1963 *Crystal Structures* vol 1 (New York: Wiley–Interscience)
[11] Kohn W and Sham L J 1965 *Phys. Rev.* **140** A1133
[12] Wills J M, Anderson P H, Nordström L, Söderlind P and Eriksson O 1999 cond-mat/9908344
[13] Dabos S, Dufour C, Benedict U and Pagès M 1987 *J. Magn. Magn. Mater.* **63–64** 661
[14] Blöchl P E, Jepsen O and Anderson O K 1994 *Phys. Rev.* B **49** 16 223
[15] Fu C L and Ho K M 1983 *Phys. Rev.* B **28** 5480

[16] Wills J M and Eriksson O 1992 *Phys. Rev.* B **45** 13 879
[17] Söderlind P, Wills J M, Boring A M, Johansson B and Eriksson O 1994 *J. Phys.: Condens. Matter* **6** 6573
[18] Ziman J M 1972 *Principle of the Theory of Solids* (Cambridge: Cambridge University Press) p 144
[19] Fournier J M and Troc R 1985 *Handbook on the Physics and Chemistry of the Actinides* vol 2, ed A J Freeman and G H Lander (Amsterdam: North-Holland) p 48
[20] Moment R L 1976 *Plutonium and Other Actinides* ed H Blank and R Lindner (Amsterdam: North-Holland) p 687
[21] Naegele J R, Cox L E and Ward J M 1993 *Proc. 23rd Journées des Actinides (Schwarzwald, 1993)*
[22] Arko A J, Joyce J J and Morales L 1999 *J. Alloys Compounds* **286** 14
[23] Svane A and Gunnarsson O 1990 *Phys. Rev. Lett.* **65** 1148
[24] Strange P, Svane A, Temmerman W M, Szotek Z and Winter H 1999 *Nature* **399** 756
[25] Petit L, Svane A, Temmerman W M and Szotek Z 2000 to be published
[26] Anisimov V I, Zaanen J and Andersen O K 1991 *Phys. Rev.* B **44** 943
[27] Savzasov S Y and Kotliar G 2000 *Phys. Rev. Lett.* **84** 3670
[28] Bouchet J, Siberchicot B, Jollet F and Pasturel A 2000 *J. Phys.: Condens. Matter* **12** 1723
[29] Price D L, Cooper B R, Lim S P and Avgin I 2000 *Phys. Rev.* B **61** 9867
[30] Eriksson O, Becker J D, Balatsky A V and Wills J M 1999 *J. Alloys Compounds* **287** 1
[31] Söderlind P, Johansson B and Eriksson O 1995 *Phys. Rev.* B **52** 1631
[32] Söderlind P, Wills J M, Johansson B and Eriksson O 1997 *Phys. Rev.* B **55** 1997